Chemical anchorage of Hydroxyapatite on 316LSS using a ZrO$_2$ interlayer for orthopedic prosthesis applications

Bermúdez-Reyes B.[*§], Contreras-García M. E.
Instituto de Investigaciones Metalúrgicas, Universidad Michoacana de San Nicolás de Hidalgo
Edificio U, Ciudad Universitaria, 58000, Morelia, Michoacán, México

Almaral-Sánchez J. L:
Universidad Autónoma de Sinaloa
Fuente de Poseidón y Prol. Ángel Flores s/n. Fracc. Las Fuentes. C.P. 81223
Los Mochis, Sinaloa, México

Espitia-Cabrera I.
Facultad de Ingeniería Química, Universidad Michoacana de San Nicolás de Hidalgo
Edificio M, Ciudad Universitaria, 58000, Morelia, Michoacán, México

Espinoza- Beltrán F. J.
Centro de Investigación y de Estudios Avanzados del I.P.N., Unidad Querétaro
Libramiento Norponiente # 2000, Frac. Real de Juriquilla,
C.P. 76230, Santiago de Querétaro, Querétaro, México

[§] *Facultad de Ingeniería Mecánica y Eléctrica, Universidad Autónoma de Nuevo León*
Av. Universidad s/n, Ciudad Universitaria, C. P. 66451
San Nicolás de los Garza, Nuevo León, México

The aim of this work is the study of the interaction mechanisms between hydroxyapatite–zirconia interface and the zirconia layer (ZrO$_2$) on a stainless steel substrate in the HA/ZrO$_2$/316LSS system. The Hydroxyapatite (HA) layer was applied by the screen printing technique on ZrO$_2$ film previously deposited by electrophoresis on 316LSS substrates. The bilayer system was thermally annealed at temperatures less than or equal to 700 °C for a maximum time of 5 minutes. The electro-deposited amorphous layers of zirconium hydroxide with a thickness about 8 μm showed good adherence to the stainless steel substrates and allowed good chemical anchorage with the HA layer after the thermal treatment, producing a thin layer of zirconia stabilized in tetragonal and monoclinic mixed phases. The thermal treatment also degraded HA layer to form calcium phosphates. The bilayer system of HA/ZrO$_2$ on 316LSS substrate ensures a good anchorage, being a good and inexpensive candidate for a protective coating in stainless steel orthopedic prostheses. This solves the low adherence between HA and 316LSS, in addition of the low cost the 316LSS prostheses as a biocompatible system with low production costs.

Keywords: Hydroxyapatite; Zirconia; Biomaterials; Bilayer coating system

1. Introduction

Human bones are composed of natural ceramic materials that show high strength and stiffness. Nevertheless, they experience loss of their mechanical properties due to sickness, natural fatigue, or wear due to age [1, 2]. In recent years there have been great advances in the development of biomaterials, mainly those used to restore defective musculoskeletal parts inside the body [3]. Different metallic, polymer, ceramic, and composite materials have been used as biomaterials inside the human body [1]. One of the widely employed structural biomaterials is SAE-AISI 316L stainless steel (316LSS), because it is considered to be a sufficiently biocompatible material. This material certainly presents degradation inside the body, and is in contact with live tissue, due to the interaction with several agents including chloride media, dynamic chemical reactions such as simultaneous oxidation-reduction, and exposure to regions without oxygen, so it only can be used for a short period of time in this bio-media [3]. In order to reduce the 316LSS degradation, modification of its surface by means of anodization, passivation, cementation, or nitridation has been recommended. The application of a bioceramic coating has been also recommended [4, 5]. Bioceramics have been used recently in order to replace many parts of the body, mainly the bones. It must be pointed out that bioceramic materials can be used in bulk as fillings or as films or coatings [6]. Zirconia has good chemical, dimensional, and mechanical stability. Young's modules of zirconia and these properties for stainless steels are very similar. On the other hand, zirconia is wear and corrosion resistant and does not present cytotoxicity in physiological media [7]. Many techniques have been used to apply

*breyes_79@yahoo.com.

Table 1. Sample identification.

Coating Sample	Label
ZrO_2 the non-annealed	Z100
ZrO_2 annealed 600 °C for 5 min	Z600
ZrO_2 annealed 650 °C for 5 min	Z650
ZrO_2 annealed 700 °C for 2 min	Z700
HA/ ZrO_2 the non-annealed	HZ200
HA/ZrO_2 annealed 600 °C for 5 min	HZ600
HA/ZrO_2 annealed 650 °C for 5 min	HZ650
HA/ZrO_2 annealed 700 °C for 2 min	HZ700

Table 2. Nomenclature for the powder samples

Powder Samples	Label
HA-ZrO_2 annealed at 600 °C for 5 min	PHAZ6005
HA-ZrO_2 annealed at 650 °C for 5 min	PHAZ6505
HA-ZrO_2 annealed at 700 °C for 2 min	PHAZ7002

zirconia coatings to 316LSS such as CVD, PVD, laser ablation, sol-gel, plasma spraying, and electrophoresis [8]. A uniform coating deposited by evaporation requires strict control of the deposition conditions and it is not possible to achieve these conditions with most of the coating techniques [9]. Electrophoresis is a simple deposition technique with which is possible to produce uniform coatings. This technique has been successfully used to obtain zirconia coatings on 316LSS substrates with good adherence properties [10, 11].

Hydroxyapatite is a bioreactive ceramic that is chemically similar to mammal bones [8]. The most important property of HA is its biocompatibility with the human body [12]. HA coatings have been obtained by sol-gel [13], plasma spraying [14], electrophoresis [15], laser ablation [16], biomimetic methods [17], RF sputtering [18], and epitaxial growth [19], among others. Screen printing techniques are proposed in this work to deposit the HA coating. This technique is simple, cheap, can be applied to different substrate shapes, and does not need special conditions (vacuum, certain atmospheres, high temperatures, etc.) [19, 20].

Previously, in another work, a procedure to produce a bilayer hybrid coating on 316LSS substrates was reported [21]. This work study the HA/ZrO2/360LSS system, the interaction mechanisms between HA-ZrO_2 layers and the ZrO_2 layer–stainless steel substrate was made. Nowadays, 316LSS prostheses are still the most used in some countries because stainless steel is a material less expensive than ceramic prosthesis. However, 316LSS is not bioactive to the bones and can release chromium and nickel debris to the blood stream metals and cause health anomalies like allergenic, mutagenic and carcinogenic reactions. 316LSS orthopedic prosthesis covered with ceramic coatings like hydroxyapatite can be biologically active coatings like hydroxyapatite, because this ceramic is compatible with the reactive biological and physical functions of the bone [3].

2. Experimental

A set of HA/ZrO2/360LSS samples was produced using the procedure described in a previous study [21]. The first layer was a zirconia film deposited by electrophoresis technique and the second layer was a hydroxyapatite coating deposited using the screen printing technique. After deposition, the HA/ZrO2/360LSS system was thermally

annealed at low temperatures for a short period of time. To analyze the evolution of the zirconia layer, a parallel set of samples without the HA layer was also obtained. The samples were labeled as follows (table 1):

Additionally, in order to dilucidate the crystallization behavior of the ZrO_2 film and its interaction with the HA and phosphates phases, powder samples were prepared from zirconium oxychloride solution hydrolysis products, which were dried and mixed with HA powder in a volume ratio of 3:1, comparable with the calculated ratio of HA:ZrO_2 on the bilayers. These samples were also studied (table 2).

These samples were analyzed by X-ray diffraction (XRD) in a Philips X'pert diffractometer, infrared spectroscopy in a PerkinElmer Spectrum GX model spectrometer in the specular reflectance mode (FTIR-reflectance), scanning electron microscopy (SEM) in a JEOL model 5910LV microscope equipped with energy dispersive X-ray spectroscopy (EDS), and atomic force microscopy (AFM) in a Veeco Nanoscope IV Dimension 3100 microscope.

3. Results and Discussion

The thermally treated ZrO_2/ coatings were observed using AFM to obtain 2 x 2 μm^2 and 10x 10 μm^2 images of their surface topography as shown in Figure 1.

Figure 1a shows the very smooth and uniform morphology of the Z100 sample. Zirconia coating Z6005 (Figure 1b) has a rough surface formed by agglomerates with a mean size of around 200 nm. A surface with bigger agglomerates, of about 2000 nm in size due to the treatment at 650 ºC, is shown in Figure 1c. Figure 1d, shows an increase in the proportion of agglomerates with a size of about 2000 nm. XRD measurements of these samples (not shown) indicated that the zirconia layer is amorphous. With the use of infrared spectroscopy analysis in these samples, it can be said that the observed agglomerates correspond to amorphous clusters of Zr–O bonds, and the vibrational modes of these bonds agree well with the tetragonal and monoclinic phases of crystalline zirconia, which may be due to the presence of zirconia with incipient crystallization (figure 2).

Stefanic et al. [22] studied the hydrolysis products of $Cr(NO_3)$ and $ZrOCl_2$, and determined that chromite stabilizes tetragonal zirconia phase. These powders were thermally treated at 400 ºC for 1 hour. They obtained chromite and tetragonal zirconia formation with a strong surface interaction between them. According to these results, the zirconia coatings are strongly bonded to the 316LSS substrates chromite. In this work the chromite on the 316LSS surface anchored and stabilized the ZrO_2 coating. In Figure 2, FTIR-reflectance spectra of the
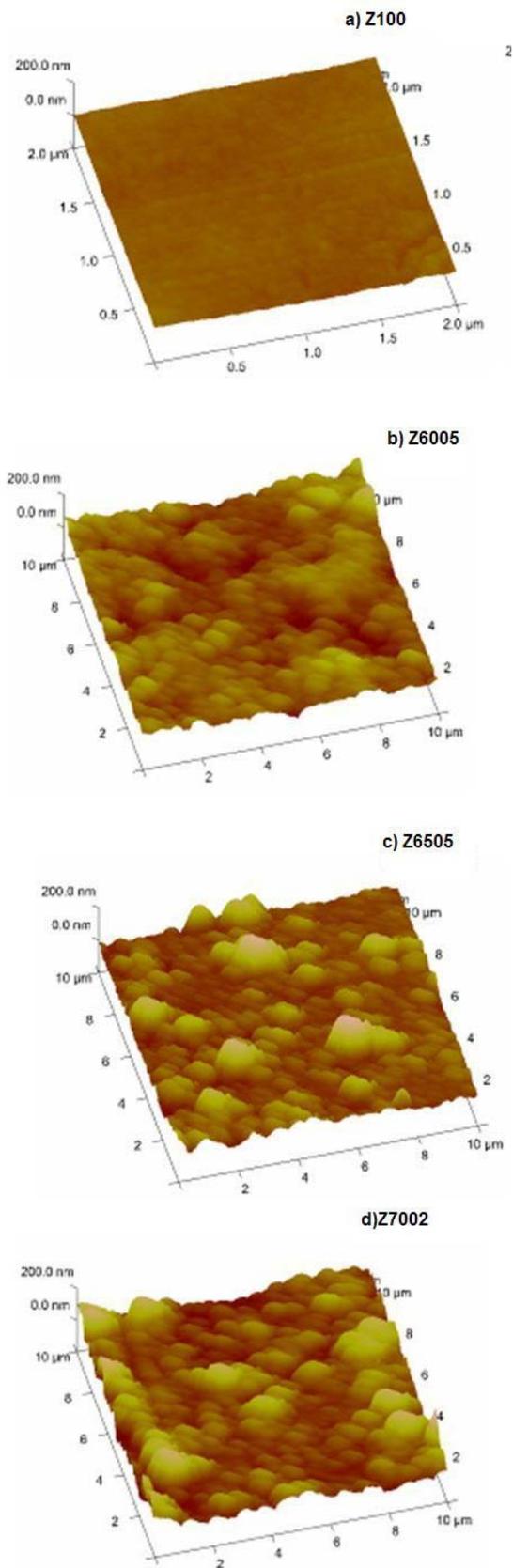
Figure 1. Topographic images of atomic force microscopy of zirconia coatings, a) after dried at 100 °C, and thermally treated at b) 600, c) 650 and d) 700 °C.

Z6005, Z6505, and Z7002 samples, some of the vibrational modes of zirconia are observed. The tetragonal and monoclinic crystalline phases of zirconia were detected. The monoclinic zirconia characteristic band was around 640 cm^{-1}, while tetragonal zirconia presents two characteristic bands localized at about 1269 and 1595 cm^{-1}. The FTIR-reflectance spectrum of the Z6505 sample presented tetragonal and monoclinic phases and another vibration band at 2338 cm^{-1} that corresponds to the mixture of tetragonal and monoclinic zirconia phases, known as martensitic zirconia, which appears at temperatures near to 650 ºC. Manríquez et al. [23] and Monterra et al. [24] reported similar FTIR-reflectance results for zirconia catalytic coatings. Moreover, during drying a martensitic phase of zirconia is formed, as reported by Tsubakino et al., who obtained this zirconia phase from $Zr(OH)_4$ powders in a temperature range from 149 °C up to 399.95 ºC [25].

To explain the results obtained by FTIR-reflectance, the chemical reactions that occur during the different steps of the process were written, and can be established as follows: during the hydrolysis reaction of the zirconium oxychloride (1), that was proposed by Mitsui [26]. After the electrophoretic deposition of $Zr(OH)_4$ + $ZrO_{2(am)}$ on the 316LSS (2), in which the chromite chemically anchored the zirconium oxyhydroxide, this occurs during drying, and during thermal treatment, forming an amorphous zirconia, according to reaction (3), where the zirconia crystallizes to tetragonal, monoclinic, and martensitic phases at relatively low temperatures and in a short time.

$$2ZrOCl_2 + 4H_2O \rightarrow Zr(OH)_4 + ZrO_{2(am)} + 4HCl$$

$$(1)$$

$$ZrO_2 \cdot ZrO(OH)_2 \cdot CrO_4 \xrightarrow{\Delta} +2ZrO_2 \cdot \cdot Cr_2O_3 + H_2O$$

$$(2)$$

$$ZrO_2 \cdot ZrO(OH)_2 \cdot Cr_2O_4 \xrightarrow{\Delta} +2ZrO_2 \cdot \cdot Cr_2O_3 + H_2O$$

$$(3)$$
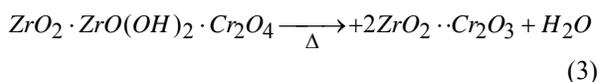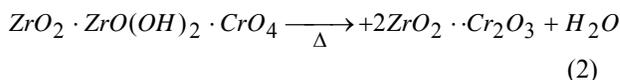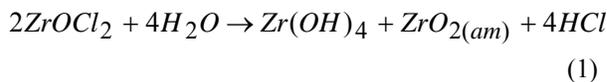
Figure 3 shows the FTIR-reflectance spectra of the HZ200, HZ6005, HZ6505, and HZ7002 samples. The FTIR-reflectance spectrum of the sample dried at 200 ºC presents the main characteristic bands of the HA at 574, 602, 962, 1575, and 3572 cm^{-1}; the bands at 863 cm^{-1} and 1416 cm^{-1} correspond to octacalcium phosphate (OCP) and to amorphous calcium phosphate (ACP), respectively. Those phosphates were produced by HA decomposition at low temperatures [27, 28].

The FTIR-reflectance spectra of the samples thermally treated at 600, 650, and 700 ºC show better defined characteristic bands corresponding to the phosphates OCP and ACP in the stretching mode of the PO^{4-} group. ACP usually appears in commercial HA as a decomposition product [27, 29]. The characteristic band of dicalcium
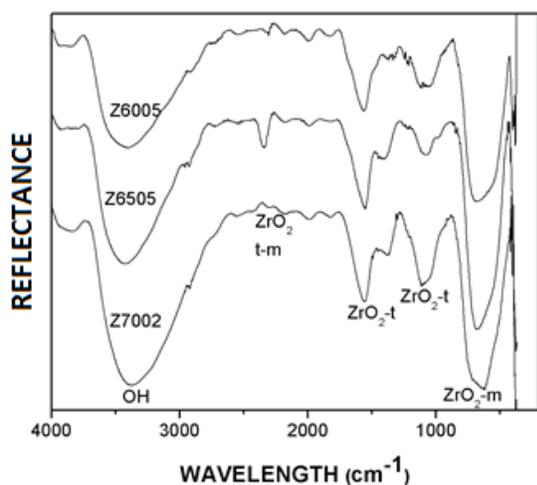
Figure 2. FTIR-reflectance spectra of the thermally treated zirconia coatings at (a) 600, (b) 650 and (c) 700 ºC.
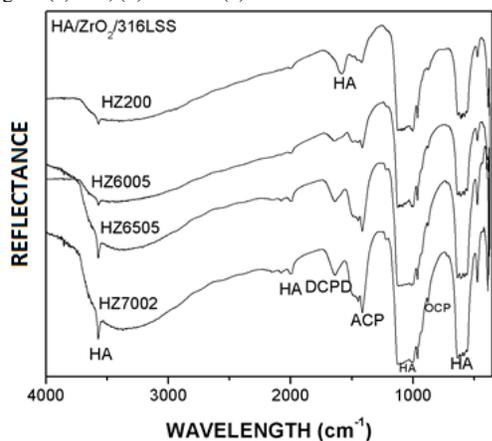
Figure 3. Infrared spectra of the thermally treated HA/ZrO2/316LSS samples at (a) 200, (b) 600, (c) 650 and (d) 700 ºC.
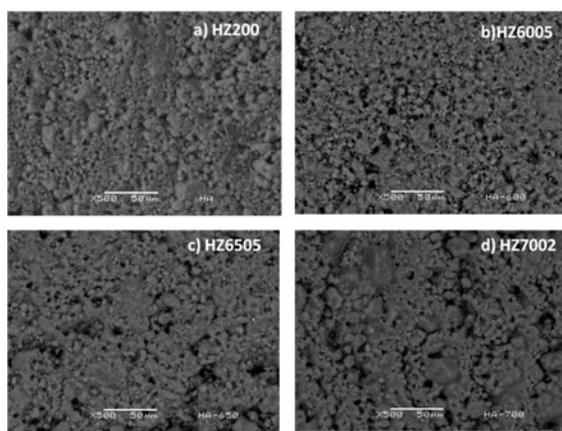
Figure 4. SEM images at 500 X of HA/ZrO2/316LSS samples, a) dried at 200 °C, and after thermal treatment at b) 600, c) 650 and d) 700 ºC.

phosphate dihydrated (DCPD) at 1630 cm^{-1} was presented from 600 ºC. This band has been reported by Joshi et al. as a product of HA decomposition in acid media [27, 30], and it is generated in the samples due to the acid atmosphere originated during the decomposition of $Zr(OH)_4$ to ZrO_2. Characteristic zirconia bands were not detected due to the thick HA layer of about 52 μm.

Scanning electron microscopy images of the morphology changes at 500μ of HA/ZrO2/316LSS samples after the thermal treatments at 200, 600, 650, and 700 °C are shown in Figure 4. The HA/ZrO$_2$ coating morphology is rough with a wide range of particle sizes due to the binding action of the propylene glycol on the HA particles, which are desirable surface characteristics allowing osteointegration [31]. The SEM image presented in Figure 4b shows the heterogeneous pore size distribution formed during the thermal treatment of the coating. Figures 4c and 4d show the porosity formation with pore sizes between 20 and 25 μm in the coatings that were thermally treated at 650 ºC for 5 min and 700 ºC for 2 min.

The pore size distribution and morphology are critical characteristics for orthopedic prosthesis applications, because they are significant properties that allow bone growth and mineral transference needed to maintain living osseous tissue [32]. According to the SEM study of the obtained coatings, the system presents two pore size distributions with two different functionalities. The pores with a size distribution between 100 and 400 μm shown in Figure 4 will allow the prosthesis to be fixed to the bone [33]. The pores with a size distribution between 1 and 25 μm (Figure 4c) will allow osteoblast growth inside them as well as to the activation of the osteointegration process [34]. With both activated mechanisms, it is possible to prevent rejection of the prosthesis and to reduce its resorption time [35]. Therefore, the screen printing technique resulted in an efficient technique to produce roughness and porous coatings using short thermal treatment times.

In order to determine the phase formation during the thermal treatment of the HA/ZrO2/316LSS coating system, the phases found at each temperature were identified by XRD. The XRD patterns of the HAZ6005, HZ6505, HZ7002, and PHZ7002 samples are given in Figure 5. The obtained diffractograms presented different crystalline phases showing the HA thermal decomposition and the zirconia coating crystallization. The observed phases were HA, OCP, DCPD, dicalcium phosphate anhydrate (DCPA), ACP, and tetragonal and monoclinic zirconia. The diffraction peaks of the monoclinic and tetragonal zirconia phases were not observed for HAZ6005, HZ6505, or HZ7002 samples. The XRD patterns for the PHZ7002 sample clearly shows the peaks due to the monoclinic and tetragonal zirconia phases, but obviously the effect is not observed due to a stainless steel substrate. Crystallization of zirconia as tetragonal and monoclinic phases at 700 °C for 2 min was promoted by the interaction between amorphous zirconia and HA. HA degrades to form OCP, DCPD, and DCPA, and a thin layer of tetragonal and monoclinic crystalline zirconia was formed. It was possible

to measure this thin layer of crystalline zirconia mean to the large surface area of the HA–ZrO$_2$ interface in the powder sample.

The HA decomposition occurred mainly at the ZrO$_2$–HA interface because, at the beginning of the thermal treatment, it was formed by amorphous ZrO$_2$ and Zr(OH)$_4$, so it had an excess of OH$^-$ ions, which causes localized basic conditions, promoting the HA decomposition to OCP. After the HA-propylenglycol paste was applied by screen printing, the dehydration during the wetting at 200 °C leads to the formation of OCP, DCPD, DCPA, ACP, and calcium oxide (CaO) [36]. Those compounds are mainly formed under basic pH and excess water conditions [37].

During thermal treatment at high temperatures (650 °C), zirconia began to crystallize and to form a solid solution with the calcium oxide product from HA decomposition, stabilizing the martensitic zirconia in the tetragonal and monoclinic phases at this temperature. Donzel et al. [38] reported zirconia stabilization at low temperatures with CaO (326–426 °C); according to them it is possible to partially stabilize zirconia in the monoclinic and tetragonal phases, originating structural vacancies, while CaO has been more widely applied to stabilize the zirconia cubic phase at higher temperatures (1326 °C) [38]. The tetragonal and monoclinic zirconia phases produced by this stabilization were obtained in this study, as was observed from XRD measurements of the PHZ6505 and PHZ7002 samples.

During thermal treatment another stabilization mechanism can be presented: the ACP stabilizes the zirconia, with the phosphate ion being responsible for this stabilization. This mechanism was reported by Spielbauer et al. [39], who obtained Zr(OH)4 powders from ZrOCl$_2$ hydrolysis and then mixed the obtained powders with potassium and sodium phosphates (both amorphous). After calcinations at 449.85 °C for 1 hour, they obtained tetragonal stabilized zirconia and the potassium and sodium phosphates were also stabilized.

According to the XRD and FTIR-reflectance results, the following reaction is proposed to explain the overall reaction at the HA/ZrO2 interface:

$$Zr(OH)_4 + ZrO_{2(am)} + 3Ca_{10}(PO_4)_6(OH)_2 \rightarrow 2ZrO_2 + Ca_8H_2(PO_4)_6 +$$

$$CaHPO_4 + CaHPO_4 \cdot 2H_2O + 2Ca_3(PO_4)_2 + 4CaO + Ca_{10}(PO_4)_6(OH)_2$$

$$(4)$$
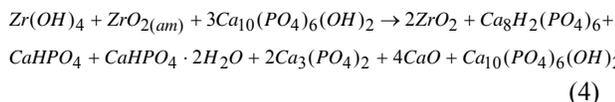
FTIR-reflectance spectrometry was also used to investigate the qualitative chemical composition of the HA/ZrO$_2$ interface, the obtained spectra are shown in Figure 6. These spectra correspond to the HZ6005, HZ6505, and HZ7002 samples after mechanical removal of the HA layer. The OCP, DCPD, and DCPA characteristic bands were detected in the interface. They are all products of HA decomposition at low temperatures [27], as explained above. An additional band at 2300 cm^{-1} corresponds to the DCPA formation generated during the DCPD dehydration [27, 30]. This result confirms the existence of the products of the proposed reaction in Equation (3).
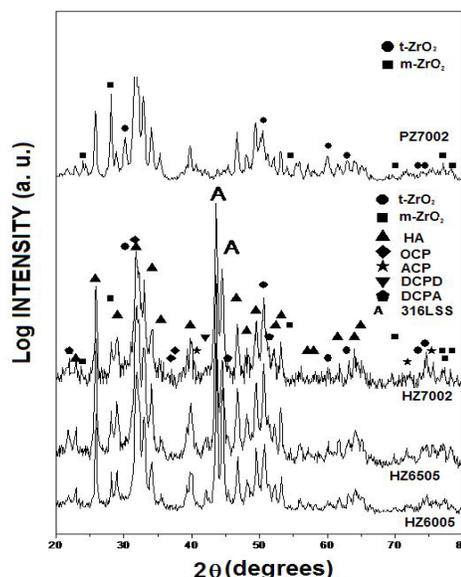
Figure 5. X-ray diffraction patterns of HA/ZrO2/316L SS samples after thermal treatments at 600, 650 and 700 °C.
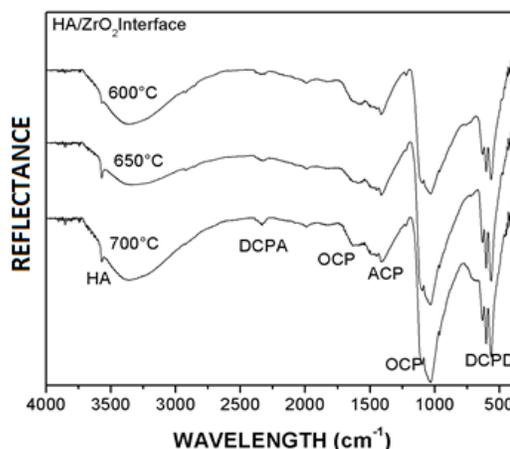
Figure 6. FTIR-reflectance HA/ZrO2/316LSS at (a) 600, (b) 650 and (c) 700 °C.
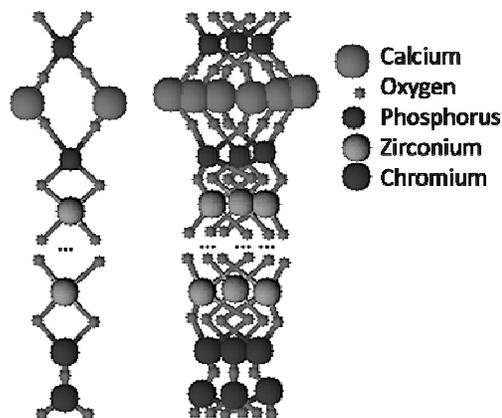
Figure 7. Chemical Anchorage Model, between HA, ZrO2 coatings and the Cr2O3 on the substrate. a) anchorage mechanism and b) coatings arrangement on 316LSS surface.

With the results obtained by XRD and FTIR-reflectance and the reaction obtained, it is possible to propose a model for the chemical anchorage between the coatings of HA and

ZrO_2 and ZrO_2 and the substrate of 316LSS, based on the proposed anchorage model by Spielbauer et al. [39] for the stabilization of ZrO_2 by phosphates. The chemical anchorage is generated by means of covalent bonds between the oxygen of the chromite of the steel and zirconia. These models, in this case, were applied to the anchorage of the ZrO_2 layer with the substrate and between the ZrO_2 layer and the HA layer, in which covalent bonds are also generated. This indicates that covalent bonds occur between the phosphate ions (that are generated from the HA decomposition during the heat treatment) and oxygen from ZrO_2; therefore all the bilayer system is chemically anchored by covalent bonds (Figure 7).

It was necessary to point out that the bioreactive property of the HA/ZrO2/316LSS system is not lost due to HA decomposition at the interface; in physiological conditions, the obtained phosphates in the interface react again to form HA in a process named natural mineralization [37]. Therefore the HA/ZrO2/316LSS system.

4. Conclusions

The interaction mechanisms between hydroxyapatite–zirconia layers and the zirconia layer–stainless steel substrate of the HA/ZrO2/316LSS system were studied. The amorphous layer of zirconia showed good adherence to the stainless steel substrates, forming chemical bonds with HA by means of producing a thin layer of stabilized ZrO2 tetragonal and monoclinic phases. HA in contact with zirconia degrades to form calcium phosphates. It was proven that the bilayer system of HA/ZrO2 on 316LSS substrate, particularly the HZ6505 sample, is a good candidate for application as a biocompatible coating for orthopedic prostheses.

Acknowledgements

References

[1]. A. Rigigutti.. Susaeta (Ediciones, Madrid, España 2002) pp.14-37.
[2]. L. L. Hench. J. Am. Ceram. Soc. **81**, 1705 (1998).
[3]. J. Helsen Jürgen Wiley, UK, 1998.
[4]. M. H. Fathi. Dental Materials, **19**, 188 (2003).
[5]. J. B. Park CRC Press, 2003.
[6]. L. L. Hench. Bioceramics: J. Am. Ceram. Soc., **74**, 1487 (1991).
[7]. C. Pconi. Biomaterials, **20**, 1 (1999).
[8]. R. Schmidt. Werlestoffverhalten in biologisschen (Systemen. Springer, Berlin, 1994).
[9]. K. Hayashi,. Biomaterials, **14**, (2003).
[10]. O. van der Biest, J. of Matter. Sci. , **39**, 779 (2004).
[11]. G. Anné, K. J. Am. Ceram. Soc. **88**(8): 2036 (2005).
[12]. B. D. Ratner. 2nd edn. (Elsevier Academic Press, USA, 2004).
[13]. P. Havibobic. J. Am. Ceram. Soc. **85**, 517 (2000).
[14]. U. Vijayalakshmi. Trends Biomater. Artif. Organs, **19**, 57 (2006).
[15]. S. M. Barinov. Biomaterials, **19**, 999 (2006).
[16]. B. Major, Bull. of the Polish Academy of Sciences Technical Sci. **52**, (2004).
[17]. A. E. Porter. J. of Mat Sci. **39**, 1895 (2004).
[18]. J. Vandiver. Biomaterial; **26**, 271 (2005).
[19]. D. E. Riemer. Solid State Technology, **8**, 45 (1998).
[20]. D. E. Riemer. Solid State Technology, **8**, 56 (1998).
[21]. B. Bermúdez-Reyes. Adv. In Tech. of Mat. And Proc. J. **9**,: 141 (2007).
[22]. G. Stefanic. Mat. Let, **36**, 240 (1998).
[23]. M. E. Manríquez. Journal of Molecular Catalysis A: Chem., **220**, 229 (1998).
[24]. C. Monterra. Langmuir, **19**, 5344 (2003).
[25]. H. Tsubakino. J. Mater. Sci., **26**, 5521 (1991).
[26]. K. Matsui. J. Am. Ceram. Soc. **80**, 1949 (2003).
[27]. S. Koutsopoulos. Wiley Periodicals **7**, 600 (2003).
[28]. M. Markovic. J. Res. Natl. Inst. Stand. Technol. **109**, 553 (2004).
[29]. G. Xu. J. Am. Chem. Soc. **123**, 2196 (2001).
[30]. V. S. Joshi. Crys. Res. Technol. **38**, 817 (2004).
[31]. L. A. Cyster. Biomaterials, **26**,697 (2005).
[32]. L. L. Hench. Bioceramics: J. Am. Ceram. Soc. **74**, 1487 (1991).
[33]. F. C. Gomes de Sousa. J. Am. Ceram. Soc. **86**, 517 (2003).
[34]. M. C. von Doerhberg. Biomaterials, 2006; **27**, 5186.
[35]. M. Mathew.J. Res. Natl. Inst. Stand. Technol., **106**, 1035 (2001).
[36]. M. S. A. Johnsson. Critical Reviews in Oral Biology and Medicine, **3**, 61 (2002).
[37]. Z. Evis. Ceram. Int. **6**, (2006).
[38]. L. Donzel. Acta Mater, **46**, 5187 (1998).
[39]. D. Speilbauer. J. Phys. Chem. B. **101**, 4681 (1998).